Operando investigation of Au-MnOx thin films with improved activity for the oxygen evolution reaction

Frydendal, Rasmus; Seitz, Linsey C.; Sokaras, Dimosthenis; Weng, Tsu-Chien; Nordlund, Dennis; Chorkendorff, Ib; Stephens, Ifan; Jaramillo, Thomas F.

Published in:
Electrochimica Acta

Link to article, DOI:
10.1016/j.electacta.2017.01.085

Publication date:
2017

Document Version
Peer reviewed version

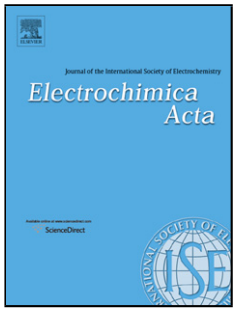

Title: Operando investigation of Au-MnO_x thin films with improved activity for the oxygen evolution reaction

Authors: Rasmus Frydendal, Linsey C. Seitz, Dimosthenis Sokaras, Tsu-Chien Weng, Dennis Nordlund, Ib Chorkendorff, Ifan E.L. Stephens, Thomas F. Jaramillo

PII: S0013-4686(17)30085-3
DOI: http://dx.doi.org/doi:10.1016/j.electacta.2017.01.085
Reference: EA 28752

To appear in: *Electrochimica Acta*

Received date: 7-11-2016
Revised date: 10-1-2017
Accepted date: 14-1-2017

Please cite this article as: Rasmus Frydendal, Linsey C.Seitz, Dimosthenis Sokaras, Tsu-Chien Weng, Dennis Nordlund, Ib Chorkendorff, Ifan E.L.Stephens, Thomas F.Jaramillo, Operando investigation of Au-MnOx thin films with improved activity for the oxygen evolution reaction, Electrochimica Acta http://dx.doi.org/10.1016/j.electacta.2017.01.085

Operando investigation of Au-MnO_x thin films with improved activity for the oxygen evolution reaction

Rasmus Frydendal,[a] Linsey C. Seitz,[b] Dimosthenis Sokaras,[c] Tsu-Chien Weng,[c] Dennis Nordlund,[c] Ib Chorkendorff,[a] Ifan E.L. Stephens,[a] Thomas F. Jaramillo,[b,c]

[a] *Section for Surface Physics and Catalysis,, Department of Physics, Building 312, Technical University of Denmark, DK-2800 Kgs. Lyngby, Denmark*

[b] *Department of Chemical Engineering, Stanford University, Stanford, California 94305, United States*

[c] *SLAC National Accelerator Laboratory, 2575 Sand Hill Road, Menlo Park, California 94025, United States*

Keywords: Water oxidation, Electrocatalysis, X-ray Absorption Spectroscopy, Operando study

Abstract

The electrochemical splitting of water holds great potential as a method for producing clean fuels by storing electricity from intermittent energy sources. The efficiency of such a process would be greatly facilitated by incorporating more active catalysts based on abundant materials for the oxygen evolution reaction. Manganese oxides are promising as catalysts for this reaction. Recent reports show that their activity can be drastically enhanced when modified with gold. Herein, we investigate highly active mixed Au-MnO_x thin films for the oxygen evolution reaction, which exhibit more than five times improvement over pure MnO_x. These films are characterized with operando X-ray Absorption Spectroscopy, which reveal that Mn assumes a higher oxidation state under reaction conditions when Au is present. The magnitude of the enhancement is correlated to the size of the Au domains, where larger domains are the more beneficial.

1. Introduction

The electrolytic production of synthetic fuels provides a promising means to average the intermittent energy supply from renewable sources. It is evident that the water oxidation reaction, known as oxygen evolution, is set to play a key role in such transformations.[1–5] Whether the goal is to produce molecular hydrogen, reduce CO_2 to hydrocarbons, or upgrade biomass, it is crucial to find a suitable source of hydrogen. For this purpose, water is ideal due to its abundance and the relative ease of water splitting, which leaves no harmful byproducts. However, the electrochemical oxygen evolution reaction, (OER), imposes a large overpotential, due to sluggish electrode kinetics.[6–9] More specifically, the difficulties in catalyzing the reaction arise from non-optimal binding energies to the three reaction intermediates, even on the most active catalysts.[10,11] This is because the binding to the reaction intermediates, *O, *OH and *OOH, correlate linearly with each other: the so called ”scaling relations”.[6,7,11,12] For all surfaces which obey these scaling relations, no catalyst will exhibit optimal binding to all three intermediates. For this reason, there is a need for novel strategies that circumvent the scaling relations and lead to catalytic surfaces with lower overpotential.[13]

A possible strategy for improving OER catalysis is to modify the surface with another material. There are several examples in the literature where such mixtures have been successful in achieving improved performance. In acidic media, ruthenium oxides mixed with either Ni or Co have been reported to be more active than the pure oxide.[14–17] Recently, Ti has also been shown to stabilize MnO_2 thin films against anodic dissolution in acidic media.[18] In alkaline media, Ni and Fe based oxides are currently utilized in commercialized electrolyser systems and combinations of the two elements have been shown to increase activity significantly.[19–22] Furthermore, Mn and Co based oxygen evolution catalysts have shown good performance in alkaline environment and various strategies have been proposed to improve their activities.[23–33] Interestingly, the presence of metallic particles or supports has a profound influence on the activity of both Mn, Co and Ni based oxide catalysts.[34–42] Mn nanoparticles deposited above or below gold

clusters can lead to a 20-fold increase in turnover frequency.[34] A possible explanation for the beneficial interaction was later proposed by two of the authors of the current manuscript on the basis of stabilized *OOH adsorption on neighboring Mn and Au sites, due to a proton transfer mechanism.[35] Recently, the role of gold nanoparticles for different MnO_x polymorphs has been investigated experimentally: it was found that the increase in OER activity could be correlated to facile formation of active Mn^{3+} sites in the presence of gold.[38] This conclusion was reached primarily from ex-situ X-ray Absorption Near Edge Spectroscopy, XANES, which indicated a lower oxidation state of Mn sites when combined with gold nanoparticles. However, judging from stability regions of the Mn-O system in aqueous environment it seems unlikely that a high concentration of Mn^{3+} should be present at the surface while turning over the OER.[43,44]

In the present study, we characterize the behavior of MnO_x under oxygen evolution conditions, using XANES to measure the Mn K-edge. To achieve a high concentration of Mn/Au neighbor sites, the samples investigated are co-sputtered thin films.

2. Experimental

Thin films of MnO_x and Au-MnO_x, with a nominal thickness of 40 nm, were prepared with reactive sputter deposition using a method previously reported.[45] The amount of material deposited was controlled by an in-chamber Quartz Crystal Microbalance, with which the deposition rates of both Mn and Au were calibrated. Mn was deposited with 140 W and Au with power dependent on the desired concentration (30 or 50 %). The deposition pressure was kept at 5 mTorr consisting of Ar and O_2 in a 25:3 ratio and the substrate temperature was 200 °C. Glassy carbon disks or wafers were used as substrates (Sigradur G, HTW GmbH), both polished to a mirror finish. To facilitate film adhesion, the glassy carbon substrates were cleaned with radio frequency (RF) sputtering in an argon atmosphere for 10 minutes prior to deposition. The glassy carbon wafer preparation has

been reported previously.[34] They were prepared to be 100-200 µm thick from GC rods and polished to an RMS roughness of less than 50 nm.

Tests of activity towards oxygen evolution were performed in a standard three electrode glass cell using 1 M KOH. A carbon rod was used as counter electrode and a Hg/HgO electrode as reference. The reference electrode potential was calibrated with a reversible hydrogen electrode (RHE) in the same electrolyte by bubbling hydrogen over a platinum mesh. All potentials are reported with respect to the RHE scale and have been corrected for Ohmic losses, evaluated with Electrochemical Impedance Spectroscopy; range 1-200000 Hz and DC potential 10 mV. The Ohmic resistance was between 5-9 Ω for all samples.

Ex-situ characterisation of the thin films was performed using X-ray Photoelectron Spectroscopy (XPS, Thermo-Fisher, base pressure of 5 x 10^{-10} mbar and X-ray source monochromatized $Al_{K\alpha}$ 1486.7 eV), Scanning Electron Microscopy (SEM, FEI, Magellan, secondary electron detector, beam voltage of 5 kV, beam current of 50 pA) and X-ray Diffraction (PANanalytical X'pert PRO equipment having an X-ray wavelength of 1.54 Å for the $Cu_{K\alpha}$ line).

Operando XAS measurements probing the Mn K-edge were performed at the SSRL Beam-line 6-2 ES2. The electrochemical setup for these measurements has been reported previously.[34,46] The cells were custom made of glass, reference electrode was based on Ag/AgCl (BASi, RE-5B), counter electrodes were carbon rods and the electrolyte was 1M KOH. The custom built glass cells allowed for the thin glassy carbon wafers to be epoxied onto an opening so that the side with catalyst material could face the electrolyte while accessible for the beam from the backside. The procedure for operando XAS measurements was as follows: First an XAS scan at Open Circuit Voltage, then at five increasingly oxidative potentials, with automatic switching triggered by the XAS software. For each of those potential steps an impedance measurement was carried out so the next

potential step could be corrected for ohmic losses. Then a linear sweep voltammetry step at 20 mV/s was started, ending at the desired potential and after 10 minutes the XAS scan would be initiated.

A double crystal Si(311) monochromator equipped with Rh-coated mirror was used to operate the beamline. Furthermore, a parabolic mirror was used to focus the beam to a spot size of 230x400 μm^2 (FWHM) at the sample position. Six spherically bent analyzer crystals of germanium ‹333› resolved the $Mn_{K\alpha}$ signal which could then be detected by an Si drift detector, SDD, in photon counting mode. The spectra presented here have all been normalised to have an edge jump of one after the linear background is subtracted. Error bars represent ±1 standard deviation from Poisson statistics and standard error propagation.

3. Results and Discussion

To investigate the beneficial interaction between Au and Mn for oxygen evolution, thin films of MnO_x mixed with two different amounts of gold were prepared. The mixed films contain 30 % or 50 % Au and are compared to pure MnO_x and a polycrystalline Au surface. The percentage values are on a total metal atomic basis, so that 30 % Au means that 30 % of the Mn is now replaced with Au.

From XPS measurements the Mn 2p and Au 4d peaks were used to evaluate the Mn:Au stoichiometry. For the 30% Au-MnO_x the XPS results for three independent samples gave an average Au concentration at the surface of 30 % with a standard deviation of 5 %, whereas for the 50% Au-MnO_x it was 52 % and a standard deviation of 4%. It should be noted that for two samples, which were tested electrochemically, a small level of Cu contamination (1-3%) was detected from XPS survey. This contamination came from the backing plate of the Mn metal target which had been used completely at the end of the study. These samples did not exhibit different electrochemical behavior and were therefore included in the mean values for the activity. XPS spectra for Mn2p, Mn3s, Au4d and O1a can be seen in the SI, Figure S1. The Mn2p½ satellite distance and Mn3s

multiplet splitting can also be used to evaluate the initial Mn:O stoichiometry.[23,47] Comparing the results obtained for as-prepared samples to literature references, indicates an Mn:O stoichiometry consistent with Mn_3O_4.

The thin films were also characterized with Glancing Angle X-ray Diffraction (GA-XRD), to investigate whether the sputter deposition method yields crystalline MnO_x or Au phases. The results for pure MnO_x can be seen in Figure 1a and the results for mixed Au-MnO_x films in Figure 1b. There are nine peaks from the MnO_x film matching with a Mn_3O_4 phase which is plausible given the low amount of oxygen present during deposition. Interestingly, the Mn_3O_4 peaks vanish for the mixed films and instead gold peaks are visible, for both concentrations. For 30 % and 50 % Au, four peaks can be identified which match with a gold face centered cubic (FCC) phase. These results clearly show that Au domains are formed. The difference between the two concentrations is the broadening of the peaks. Using Scherrers equation it is possible to estimate and compare the coherent Au domain size for the two films based on this broadening. For 30 % Au the domains are approximately 2 nm while for 50 % Au they are 3 nm. For details regarding domain size estimation, see SI. It is also possible that microstrain in the gold domains could influence the peak broadening, but the estimation is meaningful as a comparison between the two very similar films.[48] The results indicate that the Au domains are small in either case, and that from 30 % to 50 %, the Au domains within the MnO_x films grow by approximately 50 %.

(Figure 1)

The characterization of surface morphology was performed with Scanning Electron Microscopy. From Figure 2a-c it is evident that the surface morphology changes with increasing gold content. The pure MnO_x consists of pyramid shaped features, whereas the mixed films are not as strongly faceted. These images also indicate that the films with Au have a slightly more open structure which could lead to a higher surface area.

(Figure 2)

The activities of these films were then characterized with cyclic voltammetry (CV) in 1 M KOH. Figure 3 shows the initial CVs and the inset shows a comparison at 400 mV overpotential.

(Figure 3)

From the electrochemical results in Figure 3 it is clear that a significant increase in current density is obtained with increased concentration of Au in the MnO_x films. Most striking is a 5-fold improvement in activity at 400 mV overpotential for the MnO_x with 50 % Au. When comparing the overpotential at the benchmark value of 10 mA/cm^2,[49,50] the presence of Au results in a 65 mV decrease in the overpotential.

The gold could improve the conductivity of the MnO_x film, however, the similar Tafel slopes of pure and mixed films indicate that differences in uncompensated Ohmic losses are not a dominant effect. Changes in the surface morphology could lead to a higher electrochemically accessible surface area. However, the pseudo capacitance measured electrochemically is considered proportional to the active area,[50] and the change in capacitance between pure MnO_x and Au(50%)-MnO_x is below a factor of two as shown in Figure S2. Alternatively, the change in morphology could lead to an improved Mn site, so that the role of gold is solely to promote a different morphology or to prevent the formation of a crystalline Mn_3O_4 phase. This hypothesis is not supported by the data reported here, which reveals a significant difference between Au(30%)-MnO_x and Au(50%)-MnO_x, despite the facts that neither show XRD features of Mn_3O_4 while exhibiting similar surface morphology as seen in by SEM.

With the XRD and XPS data a simple model can be made to estimate how many Mn-Au interacting sites are present for the two concentrations. Here we will use the assumption that domain size (2 or 3 nm) can be used as particle size for perfectly spherical gold particles distributed on a flat Mn_3O_4 surface. The actual particle size

could differ from the domain size. If we assume the circumference of such particles is proportional to the number of Mn-Au interacting sites, then the Au(50%)-MnO_x should have approximately 1.3 times more of such sites than Au(30%)-MnO_x. Nonetheless, this increase in interacting sites is not enough to explain the factor three increase measured in current density between these two samples. For details on this model see supporting information.

With such an improvement, it is of great interest to understand the interactions between Au and MnO_x under reaction conditions. Operando XANES characterisation of the thin films was therefore carried out, specifically probing the Mn K-edge and Au L_{III}-edge while applying more oxidative potentials in 1 M KOH. In Figure 4a-c the Mn K-edge spectra are shown for each of the three Au concentrations, 0 %, 30 % and 50 %, respectively.

(Figure 4)

In Figure 4a a slight change in the Mn K-edge can be observed with a gradual increase in potential. At more positive potentials, the overall edge shifts towards higher energies, which is consistent with a small degree of oxidation of the Mn atoms, as expected from applying an oxidizing potential. For the samples with Au incorporated, Figures 4b and c, the same overall trend can be seen; at increasing potentials the edge shifts towards higher energies. However, the change is significantly more drastic for the mixed films compared to the pure MnO_x sample. Additionally, two specific features should be noted. The shoulders visible around 6548 and 6552.5 eV for the initial measurements disappear for the films with Au, while they are still visible for pure MnO_x, even at 1.65 V. These two shoulders are normally seen for Mn oxides in lower oxidation states, Mn^{2+}.[51,52] Another feature is the pre-edge located around 6540.5 eV for the dry measurements. For the pure MnO_x sample there is little to no change in the pre-edge, whereas for the mixed films a very clear splitting into two peaks is seen for both concentrations after approximately 1 V. This pre-edge splitting, has been observed previously on several different types of Mn compounds, to oxidation states of 3+ or higher.[52] However, Mn compounds with the same oxidation state can exhibit very different K-edge features depending on the local structure and due to the fact that mixed oxidation states can be present at the same time.[53] To account for such a possibility, we analyze the overall shift of the edge using a moment method where we calculate the weighted integral of the spectrum.[54] The results of that analysis are shown in Figure 4d. Consistent with the interpretations described above, this analysis shows that the incorporation of Au leads to a significant shift of the Mn K-edge towards higher energies. Even at the open circuit voltage (OCV) conditions a clear difference is observed between the pure MnO_x and the mixed films. At the highest potential, 1.65 V, the mixed films have a Mn K-edge shifted 1 eV higher than the pure MnO_x. It is unlikely that the Mn exists in a single oxidation state based on the data presented here. We emphasize, that since the Mn K-edge energies are in the hard X-ray regime, the entire bulk of the film is contributing to the signal, together with the surface

atoms. We expect the electrochemically active surface Mn atoms to be more oxidized when the potential is increased, compared to the bulk atoms.

The Au L_{III}-edge was also measured for the samples containing gold, and the resulting spectra are shown in Figure 5a and b. At OCV, Figure 5a, the spectra for Au(30%)-MnO_x and Au(50%)-MnO_x are almost identical. However, at 1.65 V_{RHE} there is a distinct increase in the white line for the lower Au concentration. A higher white line indicates that the Au is oxidized.[55,56] From the Pourbaix diagram of gold, the oxidation to a +3 state can occur at potentials close to 1.46 V_{RHE} so it is not a surprising feature. Nevertheless it is a feature that is missing for the higher concentration of Au, indicating that a significant amount of the gold in the 30% sample is oxidized, which could be attributed in part to its smaller domain size compared the Au(50%)-MnO_x sample.

(Figure 5)

Since the XANES results show a higher oxidation for MnO_x films mixed with gold, it raises the question; why does a higher oxidation state lead to higher OER activity? One possible reason is that the binding energies for Mn sites in a higher oxidation state are closer to the optimal strengths. This notion can be justified with the DFT calculations reported previously where MnO_2 is predicted to have a lower overpotential than Mn_2O_3, Mn_3O_4 and MnO.[10,43] However, at oxidative potentials relevant for OER there will be a thermodynamic driving force toward forming MnO_2 regardless of the initial oxide phase. We can compare the activity of the pure MnO_x reported here, which has an Mn_3O_4 phase to begin with, to a previously reported MnO_x thin film prepared as MnO_2 since both samples have been made by sputter deposition and with the same nominal thickness.[45] At 400 mV overpotential for OER the current measured for MnO_x in Mn_3O_4 phase is 0.76 mA/cm^2 while the MnO_2 showed a slightly lower current of 0.69 mA/cm^2. Instead, for the Au(50%)-MnO_x the OER current is more than five times higher, indicating a different type of active site altogether.

It is also interesting that the two Au concentrations result in very similar Mn oxidation state from the Operando XANES, while the activity enhancement is much more significant at 50 % Au. An observed difference between the two concentrations is the Au domain size, which was larger by 50 %. Furthermore, the Au L_{III}-edge spectra revealed that the sample with 30% gold was significantly oxidized at high potentials, whereas the sample with 50 % gold was not. Assuming that the domain size estimated with XRD is a suitable measure of the particle size, it should be noted that size effects for oxygen electrochemistry is very significant in the range of 1-5 nm.[57] A possible explanation for the observations is that a certain size of Au particles is necessary for the full enhancement. This enhancement could be related to the type of Au sites available at the surface of such particles during oxygen turnover.[35,58] Greeley et al. have reported that the binding to OER intermediates for Au surfaces is stronger for undercoordinated sites.[59] Specifically, *OH binding to Au(211) was 0.17 eV stronger than to Au(100). Furthermore, the number of undercoordinated sites for Au particles increases dramatically when the size of particles is decreased from 5 to 1 nm.[58] For the smaller Au domains, this is consistent with oxidation at more cathodic potentials as observed with XAS. This could explain differences with previous studies that employed an average Au size of 4 nm,[38] likely to contain fewer undercoordinated sites. These observations indirectly indicate that Au terrace sites might be important for interactions with Mn oxides. From a recent theoretical model, *OH adsorbed on the terrace sites of bulk Au(111) was proposed as a proton acceptor.[35] A particle size dependency on the activity could suggest that these sites are indeed important and play a role in the reaction mechanism.

However, to fully establish such an effect more specific measurements must be carried out. From the operando measurements reported herein, however, it is clear that gold promotes the activity towards OER and leads to higher oxidation state of Mn under reaction conditions. In future studies it would be of great interest to bring about a similar beneficial effect without resorting to precious metals.

4. Conclusion

In this study we have investigated mixed Au-MnO_x films as catalysts for the oxygen evolution reaction. Films with 30 % Au exhibited modest increase in current density over a pure MnO_x film. At 50 % Au, more than five times higher current densities were measured. From X-ray Diffraction measurements it was found that the pure MnO_x has a clear Mn_3O_4 phase and when adding Au, it forms particles in the MnO_x matrix, with sizes dependent on the Au concentration. At 30 % Au the crystallite size was approximately 2 nm, while at 50 % Au it increased to 3 nm. The films were studied with Operando X-ray Absorption Spectroscopy where the Mn K-edge and Au L_{III}-edge were probed as a function of electrochemical potential. At increasingly anodic potentials all films showed a shift of the Mn K-edge towards higher photon energies. However, the films with Au showed a significantly larger shift, indicating that the surface and bulk Mn atoms on average reach a higher oxidation state. The Au L_{III}-edge revealed that at a low Au concentration, 30 %, significant oxidation could be seen, which was not the case at 50 %. The combined study suggests that a beneficial interaction between Mn oxide and Au depends on more than just the number of neighboring Mn-Au sites. The results indicate that the morphology of Au particles or type of Au sites available next to OER active Mn sites has a strong impact on the increase in OER activity.

Acknowledgements

The authors gratefully acknowledge financial support from the Danish Ministry of Science's UNIK initiative, Catalysis for Sustainable Energy. This work was partially supported by the US Department of Energy, Basic Energy Science through the SUNCAT Center for Interface Science and Catalysis. LCS received fellowship support from the DARE Doctoral Fellowship supported by the Vice Provost for Graduate Education at Stanford University. Part of this work was performed at the Stanford Nano Shared Facilities (SNSF). Use of the Stanford Synchrotron Radiation Lightsource (SSRL), SLAC National Accelerator Laboratory, is supported by the U.S. Department of Energy, Office of Science, Office of Basic Energy Sciences under Contract No. DE-AC02-76SF00515. This work was supported by a research grant (9455) from VILLUM FONDEN.

References

[1] J. Greeley, N.M. Markovic, The road from animal electricity to green energy: combining experiment and theory in electrocatalysis, Energy Environ. Sci. 5 (2012) 9246–9256. doi:10.1039/c2ee21754f.

[2] H.A. Gasteiger, N.M. Markovic, Just a Dream—or Future Reality?, Science. 324 (2009) 48–50.

[3] K. Maeda, K. Domen, Photocatalytic water splitting: Recent progress and future challenges, J. Phys. Chem. Lett. 1 (2010) 2655–2661. doi:10.1021/jz1007966.

[4] N.S. Lewis, D.G. Nocera, Powering the planet: chemical challenges in solar energy utilization., Proc. Natl. Acad. Sci. U. S. A. 103 (2006) 15729–35. doi:10.1073/pnas.0603395103.

[5] E. Fabbri, A. Habereder, K. Waltar, R. Kotz, T. Schmidt, Developments and perspectives of oxide-based catalysts for the oxygen evolution reaction, Catal. Sci. Technol. 4 (2014) 3800–3821. doi:10.1039/C4CY00669K.

[6] J. Rossmeisl, A. Logadottir, J.K. Nørskov, Electrolysis of water on (oxidized) metal surfaces, Chem. Phys. 319 (2005) 178–184. doi:10.1016/j.chemphys.2005.05.038.

[7] J. Rossmeisl, Z.-W. Qu, H. Zhu, G.-J. Kroes, J.K. Nørskov, Electrolysis of water on oxide surfaces, J. Electroanal. Chem. 607 (2007) 83–89. doi:10.1016/j.jelechem.2006.11.008.

[8] S. Trasatti, ELECTROCATALYSIS BY OXIDES -- ATTEMPT AT A UNIFYING APPROACH, J. Electroanal. Chem. 111 (1980) 125–131.

[9] I. Katsounaros, S. Cherevko, A.R. Zeradjanin, K.J.J. Mayrhofer, Oxygen electrochemistry as a

cornerstone for sustainable energy conversion., Angew. Chem. Int. Ed. Engl. 53 (2014) 102–21. doi:10.1002/anie.201306588.

[10] I.C. Man, H.-Y. Su, F. Calle-Vallejo, H.A. Hansen, J.I. Martínez, N.G. Inoglu, et al., Universality in Oxygen Evolution Electrocatalysis on Oxide Surfaces, ChemCatChem. 3 (2011) 1159–1165. doi:10.1002/cctc.201000397.

[11] M.T.M. Koper, Thermodynamic theory of multi-electron transfer reactions: Implications for electrocatalysis, J. Electroanal. Chem. 660 (2011) 254–260. doi:10.1016/j.jelechem.2010.10.004.

[12] F. Abild-Pedersen, J. Greeley, F. Studt, J. Rossmeisl, T. Munter, P. Moses, et al., Scaling Properties of Adsorption Energies for Hydrogen-Containing Molecules on Transition-Metal Surfaces, Phys. Rev. Lett. 99 (2007) 16105. doi:10.1103/PhysRevLett.99.016105.

[13] A.D. Doyle, J.H. Montoya, A. Vojvodic, Improving Oxygen Electrochemistry through Nanoscopic Confinement, ChemCatChem. 94025 (2015) 738–742. doi:10.1002/cctc.201402864.

[14] T. Reier, M. Oezaslan, P. Strasser, Electrocatalytic Oxygen Evolution Reaction (OER) on Ru, Ir, and Pt Catalysts: A Comparative Study of Nanoparticles and Bulk Materials, ACS Catal. 2 (2012) 1765–1772. doi:10.1021/cs3003098.

[15] N.B. Halck, V. Petrykin, P. Krtil, J. Rossmeisl, Beyond the volcano limitations in electrocatalysis - oxygen evolution reaction., Phys. Chem. Chem. Phys. 16 (2014) 13682–13688. doi:10.1039/c4cp00571f.

[16] V. Petrykin, K. Macounová, M. Okube, S. Mukerjee, P. Krtil, Local structure of Co doped RuO2 nanocrystalline electrocatalytic materials for chlorine and oxygen evolution, Catal. Today. 202 (2013) 63–69. doi:10.1016/j.cattod.2012.03.075.

[17] K. Macounová, J. Jirkovský, M. V. Makarova, J. Franc, P. Krtil, Oxygen evolution on Ru1-xNixO2-y nanocrystalline electrodes, J. Solid State Electrochem. 13 (2009) 959–965. doi:10.1007/s10008-008-0624-1.

[18] R. Frydendal, E.A. Paoli, I. Chorkendorff, J. Rossmeisl, I.E.L. Stephens, Toward an Active and Stable Catalyst for Oxygen Evolution in Acidic Media: Ti-Stabilized MnO2, Adv. Energy Mater. n/a (2015). doi:10.1002.aenm201500991.

[19] L. Trotochaud, S.L. Young, J.K. Ranney, S.W. Boettcher, Nickel-iron oxyhydroxide oxygen-evolution electrocatalysts: the role of intentional and incidental iron incorporation., J. Am. Chem. Soc. 136 (2014) 6744–53. doi:10.1021/ja502379c.

[20] D. Friebel, M.W. Louie, M. Bajdich, K.E. Sanwald, Y. Cai, A.M. Wise, et al., Identification of Highly Active Fe Sites in (Ni,Fe)OOH for Electrocatalytic Water Splitting, J. Am. Chem. Soc. 137 (2015) 1305–1313. doi:10.1021/ja511559d.

[21] F. Song, X. Hu, Exfoliation of layered double hydroxides for enhanced oxygen evolution catalysis, Nat. Commun. 5 (2014) 1–9. doi:10.1038/ncomms5477.

[22] O. Diaz-Morales, I. Ledezma-Yanez, M.T.M. Koper, F. Calle-Vallejo, Guidelines for the Rational Design of Ni-Based Double Hydroxide Electrocatalysts for the Oxygen Evolution Reaction, ACS Catal. 5 (2015)

5380–5387. doi:10.1021/acscatal.5b01638.

[23] Y. Gorlin, T.F. Jaramillo, A bifunctional nonprecious metal catalyst for oxygen reduction and water oxidation., J. Am. Chem. Soc. 132 (2010) 13612–13614. doi:10.1021/ja104587v.

[24] H. Dau, C. Limberg, T. Reier, M. Risch, S. Roggan, P. Strasser, The Mechanism of Water Oxidation: From Electrolysis via Homogeneous to Biological Catalysis, ChemCatChem. 2 (2010) 724–761. doi:10.1002/cctc.201000126.

[25] F. Jiao, H. Frei, Nanostructured Cobalt Oxide Clusters in Mesoporous Silica as Efficient Oxygen-Evolving Catalysts, Angew. Chemie. 48 (2009) 1841–1844. doi:10.1002/ange.200805534.

[26] J. Suntivich, K.J. May, H.A. Gasteiger, J.B. Goodenough, Y. Shao-Horn, A Perovskite Oxide Optimized for Oxygen Evolution Catalysis from Molecular Orbital Principles, Science (80-.). 334 (2011) 1383–1385. doi:10.1126/science.1212858.

[27] A. Grimaud, K.J. May, C.E. Carlton, Y.-L. Lee, M. Risch, W.T. Hong, et al., Double perovskites as a family of highly active catalysts for oxygen evolution in alkaline solution., Nat. Commun. 4 (2013) 2439. doi:10.1038/ncomms3439.

[28] K. Mette, A. Bergmann, J.-P. Tessonnier, M. Hävecker, L. Yao, T. Ressler, et al., Nanostructured Manganese Oxide Supported on Carbon Nanotubes for Electrocatalytic Water Splitting, ChemCatChem. 4 (2012) 851–862. doi:10.1002/cctc.201100434.

[29] D.G. Nocera, The artificial leaf., Acc. Chem. Res. 45 (2012) 767–76. doi:10.1021/ar2003013.

[30] J. Rosen, G.S. Hutchings, F. Jiao, Ordered Mesoporous Cobalt Oxide as Highly Efficient Oxygen Evolution Catalyst., J. Am. Chem. Soc. 135 (2013) 4516–4521. doi:10.1021/ja400555q.

[31] W.T. Hong, M. Risch, K.A. Stoerzinger, A. Grimaud, J. Suntivich, Y. Shao-Horn, Toward the rational design of non-precious transition metal oxides for oxygen electrocatalysis, Energy Environ. Sci. 8 (2015) 1404–1427. doi:10.1039/C4EE03869J.

[32] R. Mohamed, X. Cheng, E. Fabbri, P. Levecque, R. Kötz, O. Conrad, et al., Electrocatalysis of perovskites: The influence of carbon on the oxygen evolution activity, J. Electrochem. Soc. 162 (2015) F579–F586. doi:10.1149/2.0861506jes.

[33] R. Subbaraman, D. Tripkovic, K.-C. Chang, D. Strmcnik, A.P. Paulikas, P. Hirunsit, et al., Trends in activity for the water electrolyser reactions on 3d M(Ni,Co,Fe,Mn) hydr(oxy)oxide catalysts., Nat. Mater. 11 (2012) 550–557. doi:10.1038/nmat3313.

[34] Y. Gorlin, C.-J. Chung, J.D. Benck, D. Nordlund, L. Seitz, T.-C. Weng, et al., Understanding Interactions between Manganese Oxide and Gold That Lead to Enhanced Activity for Electrocatalytic Water Oxidation., J. Am. Chem. Soc. 136 (2014) 4920–4926. doi:10.1021/ja407581w.

[35] R. Frydendal, M. Busch, N.B. Halck, E. a. Paoli, P. Krtil, I. Chorkendorff, et al., Enhancing Activity for the Oxygen Evolution Reaction: The Beneficial Interaction of Gold with Manganese and Cobalt Oxides, ChemCatChem. 7 (2015) 149–154. doi:10.1002/cctc.201402756.

[36] X. Lu, Y.H. Ng, C. Zhao, Gold nanoparticles embedded within mesoporous cobalt oxide enhance electrochemical oxygen evolution., ChemSusChem. 7 (2014) 82–86. doi:10.1002/cssc.201300975.

[37] B.S. Yeo, A.T. Bell, Enhanced activity of gold-supported cobalt oxide for the electrochemical evolution of oxygen., J. Am. Chem. Soc. 133 (2011) 5587–5593. doi:10.1021/ja200559j.

[38] C. Kuo, W. Li, L. Pahalagedara, A.M. El-Sawy, D. Kriz, N. Genz, et al., Understanding the Role of Gold Nanoparticles in Enhancing the Catalytic Activity of Manganese Oxides in Water Oxidation Reactions, Angew. Chemie Int. Ed. 127 (2014) 2375–2380. doi:10.1002/anie.201407783.

[39] M.S. El-Deab, M.I. Awad, A.M. Mohammad, T. Ohsaka, Enhanced water electrolysis: Electrocatalytic generation of oxygen gas at manganese oxide nanorods modified electrodes, Electrochem. Commun. 9 (2007) 2082–2087. doi:10.1016/j.elecom.2007.06.011.

[40] B.S. Yeo, A.T. Bell, In Situ Raman Study of Nickel Oxide and Gold-Supported Nickel Oxide Catalysts for the Electrochemical Evolution of Oxygen, J. Phys. Chem. C. 116 (2012) 8394–8400. doi:10.1021/jp3007415.

[41] L.C. Seitz, T.J.P. Hersbach, D. Nordlund, T.F. Jaramillo, Enhancement Effect of Noble Metals on Manganese Oxide for the Oxygen Evolution Reaction, J. Phys. Chem. Lett. 6 (2015) 4178–4183. doi:10.1021/acs.jpclett.5b01928.

[42] J.W.D. Ng, M. García-Melchor, M. Bajdich, P. Chakthranont, C. Kirk, A. Vojvodic, et al., Gold-supported cerium-doped NiOx catalysts for water oxidation, Nat. Energy. 1 (2016) 16053.

[43] H.-Y. Su, Y. Gorlin, I.C. Man, F. Calle-Vallejo, J.K. Nørskov, F. Jaramillo, et al., Identifying active surface phases for metal oxide electrocatalysts: a study of manganese oxide bi-functional catalysts for oxygen reduction and water oxidation catalysis., Phys. Chem. Chem. Phys. 14 (2012) 14010–14022. doi:10.1039/c2cp40841d.

[44] M. Pourbaix, Atlas of Electrochemical Equilibria in Aqueous Solutions, 1st ed., Pergamon Press, 1966.

[45] R. Frydendal, E.A. Paoli, B.P. Knudsen, B. Wickman, P. Malacrida, I.E.L. Stephens, et al., Benchmarking the Stability of Oxygen Evolution Reaction Catalysts: The Importance of Monitoring Mass Losses, ChemElectroChem. 1 (2014) 2075–2081. doi:10.1002/celc.201402262.

[46] Y. Gorlin, B. Lassalle-Kaiser, J.D. Benck, S. Gul, S.M. Webb, V.K. Yachandra, et al., In situ X-ray absorption spectroscopy investigation of a bifunctional manganese oxide catalyst with high activity for electrochemical water oxidation and oxygen reduction., J. Am. Chem. Soc. 135 (2013) 8525–8534. doi:10.1021/ja3104632.

[47] V. Di Castro, G. Polzonetti, XPS study of MnO oxidation, J. Electron Spectros. Relat. Phenomena. 48 (1989) 117–123. doi:10.1016/0368-2048(89)80009-X.

[48] A.J.C. Langford, J.I. and Wilson, Scherrer after Sixty Years: A Survey and Some New Results in the Determination of Crystallite Size, J. Appl. Crystallogr. 11 (1978) 102–113. doi:doi:10.1107/S0021889878012844.

[49] M.G. Walter, E.L. Warren, J.R. McKone, S.W. Boettcher, Q. Mi, E.A. Santori, et al., Solar water splitting

cells., Chem. Rev. 110 (2010) 6446–6473. doi:10.1021/cr1002326.

[50] C.C.L. McCrory, S. Jung, J.C. Peters, T.F. Jaramillo, Benchmarking heterogeneous electrocatalysts for the oxygen evolution reaction., J. Am. Chem. Soc. 135 (2013) 16977–87. doi:10.1021/ja407115p.

[51] F. Jiao, H. Frei, Nanostructured manganese oxide clusters supported on mesoporous silica as efficient oxygen-evolving catalysts., Chem. Commun. 46 (2010) 2920–2922. doi:10.1039/b921820c.

[52] F. Farges, Ab initio and experimental pre-edge investigations of the Mn K-edge XANES in oxide-type materials, Phys. Rev. B - Condens. Matter Mater. Phys. 71 (2005) 1–14. doi:10.1103/PhysRevB.71.155109.

[53] A. Manceau, M.A. Marcus, S. Grangeon, Determination of Mn valence states in mixed-valent manganates by XANES spectroscopy, Am. Mineral. 97 (2012) 816–827. doi:10.2138/am.2012.3903.

[54] T.C. Weng, W.Y. Hsieh, E.S. Uffelman, S.W. Gordon-Wylie, T.J. Collins, V.L. Pecoraro, et al., XANES evidence against a manganyl species in the S3 state of the oxygen-evolving complex, J. Am. Chem. Soc. 126 (2004) 8070–8071. doi:10.1021/ja0494104.

[55] P. Haider, J.D. Grunwaldt, R. Seidel, A. Baiker, Gold supported on Cu-Mg-Al and Cu-Ce mixed oxides: An in situ XANES study on the state of Au during aerobic alcohol oxidation, J. Catal. 250 (2007) 313–323. doi:10.1016/j.jcat.2007.07.001.

[56] Y. Konishi, T. Tsukiyama, N. Saitoh, T. Nomura, S. Nagamine, Y. Takahashi, et al., Direct determination of oxidation state of gold deposits in metal-reducing bacterium Shewanella algae using X-ray absorption near-edge structure spectroscopy (XANES)., J. Biosci. Bioeng. 103 (2007) 568–571. doi:10.1263/jbb.103.568.

[57] F.J. Perez-Alonso, D.N. McCarthy, A. Nierhoff, P. Hernandez-Fernandez, C. Strebel, I.E.L. Stephens, et al., The effect of size on the oxygen electroreduction activity of mass-selected platinum nanoparticles., Angew. Chem. Int. Ed. Engl. 51 (2012) 4641–3. doi:10.1002/anie.201200586.

[58] S.H. Brodersen, U. Grønbjerg, B. Hvolbæk, J. Schiøtz, Understanding the catalytic activity of gold nanoparticles through multi-scale simulations, J. Catal. 284 (2011) 34–41. doi:10.1016/j.jcat.2011.08.016.

[59] J. Greeley, J. Rossmeisl, A. Hellman, J.K. Nørskov, Theoretical Trends in Particle Size Effects for the Oxygen Reduction Reaction, Zeitschrift Für Phys. Chemie. 221 (2007) 1209–1220. doi:10.1524/zpch.2007.221.9-10.1209.

Figures

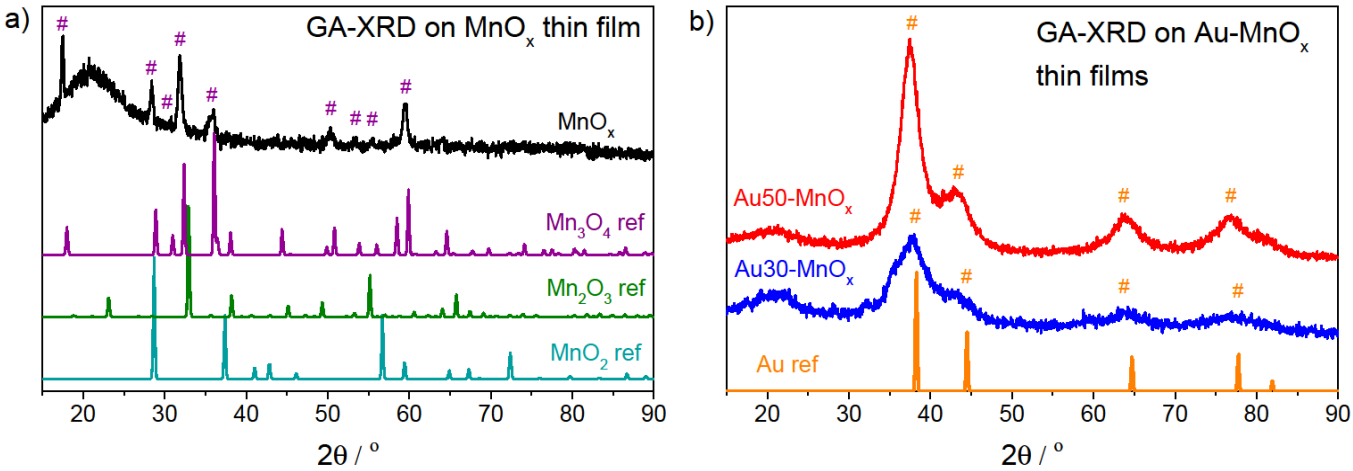

Figure 1. a) X-ray Diffraction for pure MnO_x film, in black, together with references for Mn_3O_4 (purple), Mn_2O_3 (green) and MnO_2 (teal). The peaks matching Mn_3O_4 lines are indicated with blue #. b) X-ray Diffraction results for Au-MnO_x films, 50% Au in red and 30 % Au in blue. A gold reference is shown in orange. The four main peaks for Au is indicated with orange #.

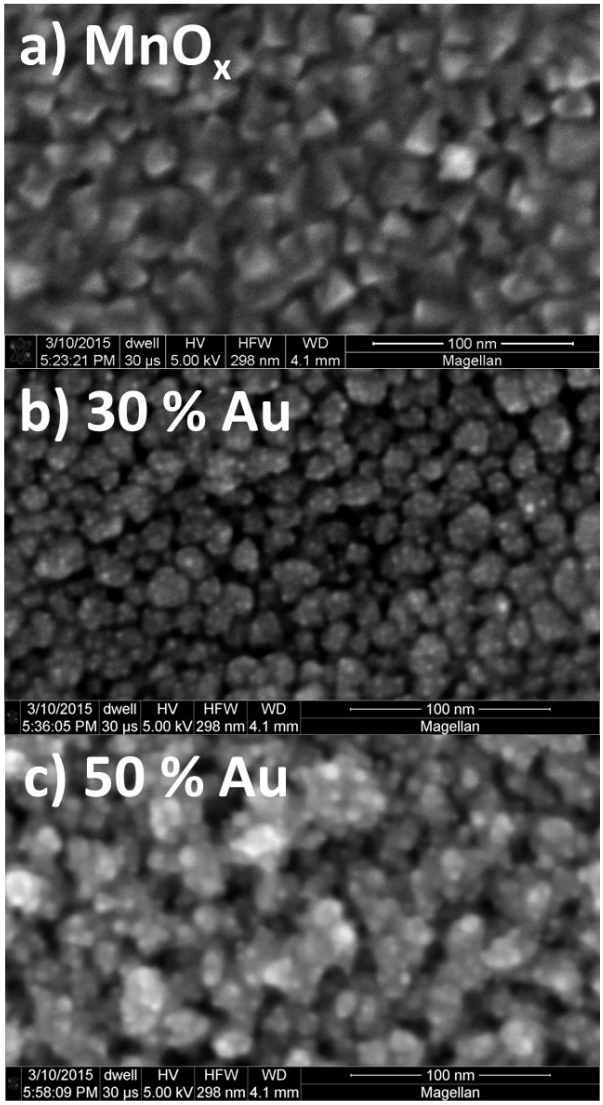

Figure 2. Scanning Electron Microscopy images for a) pure MnO_x b) MnO_x with 30 % Au and c) MnO_x with 50 % Au.

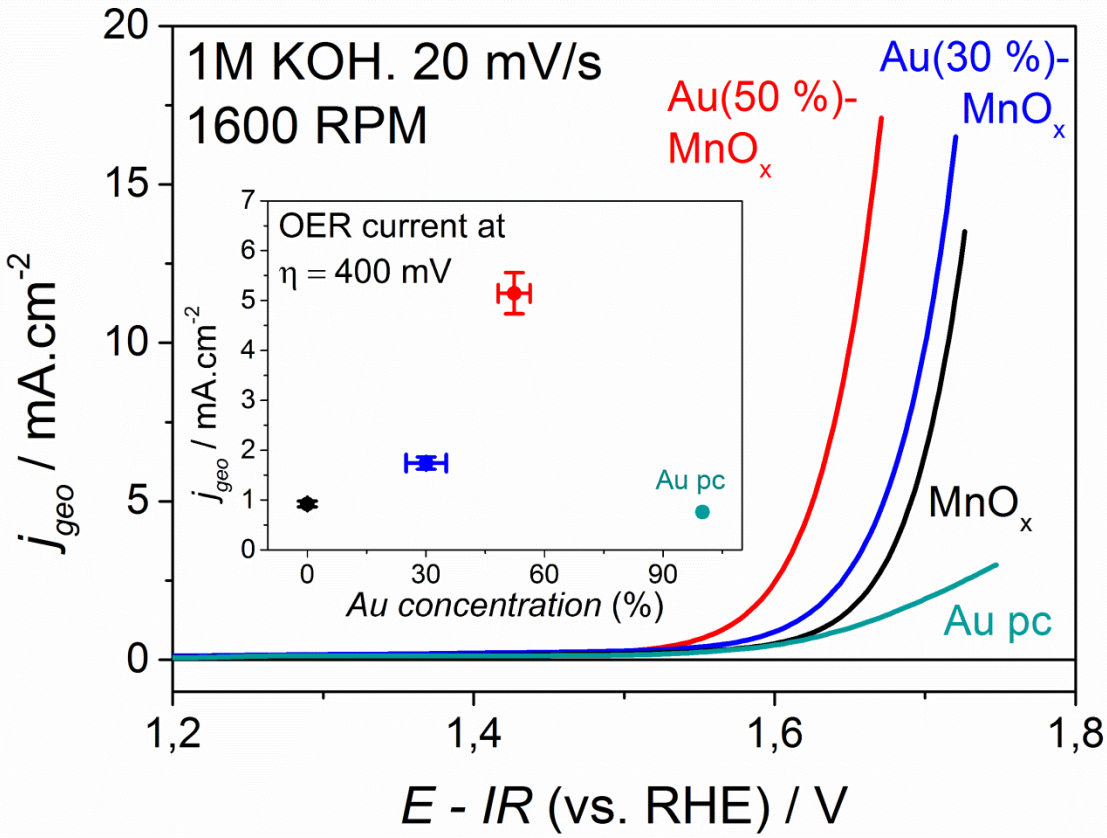

Figure 3. Initial cyclic voltammetry for MnO_x films with 0, 30 and 50 % Au and for an Au pc (polycrystalline sample). The results were obtained for Rotating Disk Electrodes which were performed in 1M KOH using a scan rate 20 mV/s and a rotation speed of 1600 RPM. Inset: At each concentration the activities are compared at an overpotential of 400 mV. The error bars are based on three independent measurements and the Au concentration is evaluated with XPS.

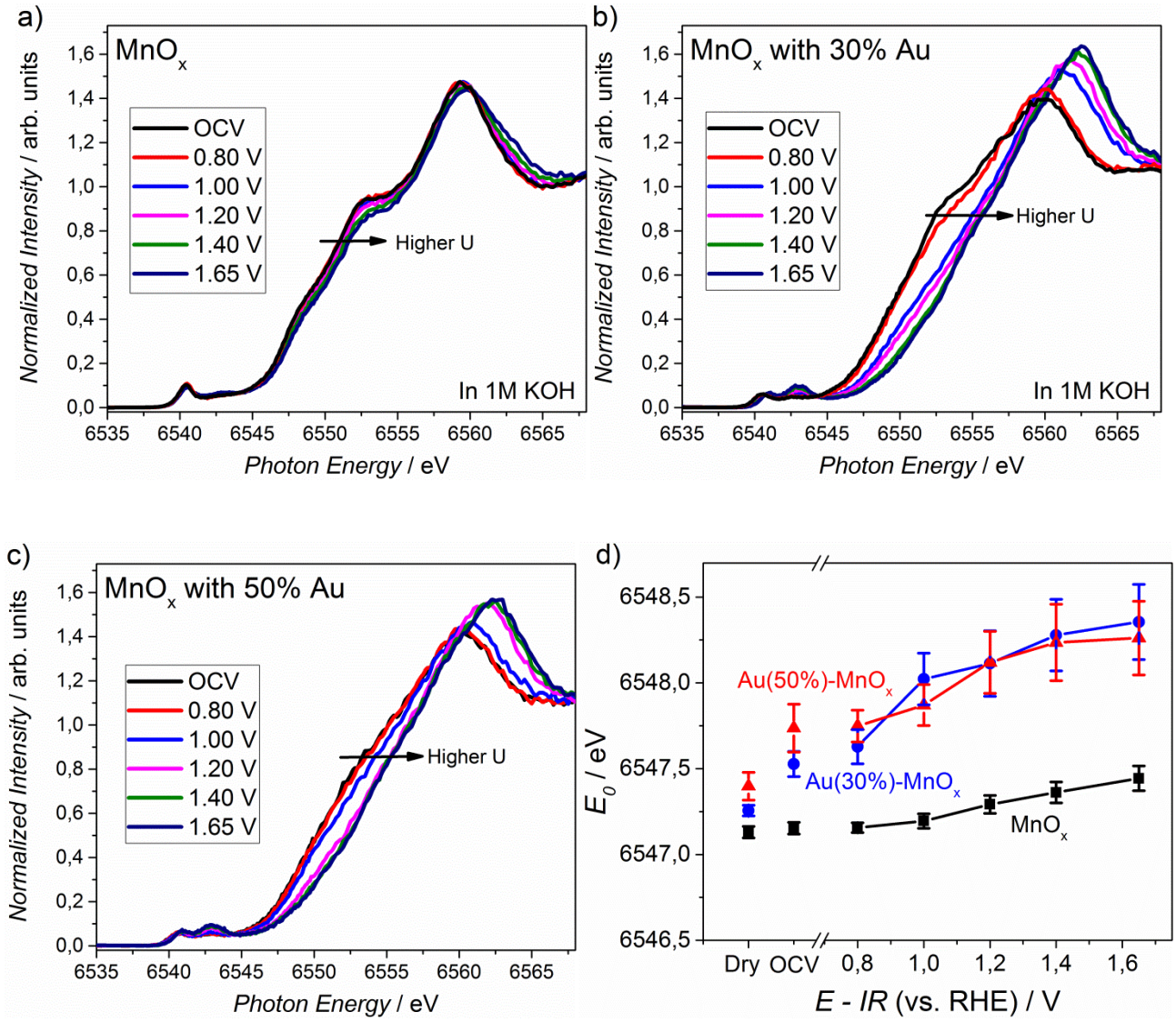

Figure 4. a) Normalised Mn K-edge results for the pure MnO_x thin film. **b)** Normalised Mn K-edge results for the MnO_x thin film with 30 % Au. **c)** Normalised Mn K-edge results for the MnO_x thin film with 50 % Au. **d)** Moment analysis of Mn K-edge data for the three thin films. This method takes into account the general shift of the K-edge features in a large energy range instead of focusing on a single feature. The error bar are based on varying the integral range in the first moment equation.

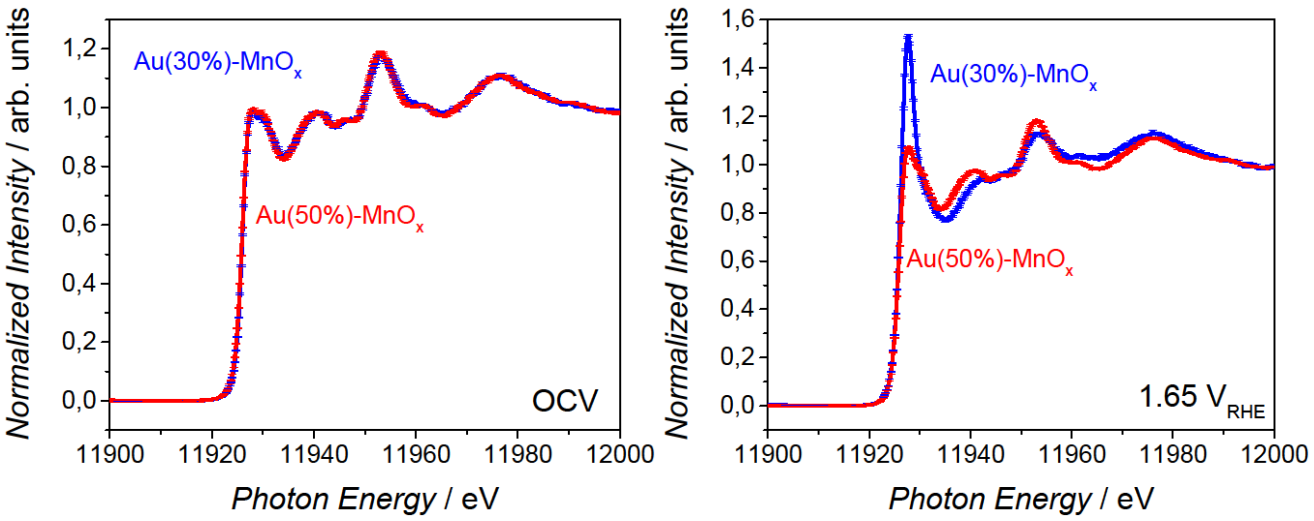

Figure 5. a) Au L_{III}-spectra for Au(30%)-MnO_x (blue) and Au(50%)-MnO_x (red) at open circuit conditions. b) Au L_{III}-spectra for Au(30%)-MnO_x (blue) and Au(50%)-MnO_x (red) at 1.65 V_{RHE}.